



In Utero Nano-Titanium Dioxide Exposure Results in Sexually Dimorphic Weight Gain and Cardiovascular Function in Offspring

Russell Hunter¹ · Teresa Gluth¹ · Ethan Meadows² · Riley Nett¹ · Victoria Nist¹ · Elizabeth Bowdridge¹

Received: 11 October 2024 / Accepted: 8 January 2025 / Published online: 21 January 2025
© The Author(s) 2025

Abstract

Engineered nanomaterials (ENM) are capable of crossing the placental barrier and accumulating in fetal tissue. Specifically, the ENM nano-titanium dioxide (nano-TiO₂), has been shown to accumulate in placental and fetal tissue, resulting in decreased birthweight in pups. Additionally, nano-TiO₂ is an established cardiac toxicant and regulator of glucose homeostasis, and exposure *in utero* may lead to serious maladaptive responses in cardiac development and overall metabolism. The current study examines weight gain and cardiac function in male and female Sprague–Dawley rats exposed to 12 mg/m³ nano-TiO₂ or filtered air for 6 non-consecutive days *in utero* between gestational days 12–19. These animals were randomly assigned to receive a grain-based or high-fat diet (60%) between postnatal weeks 12–24 to examine the propensity for weight gain and cardiac response as adults. Our results show a sexually dimorphic response to weight gain with male rats gaining more weight after high-fat diet following *in utero* nano-TiO₂ exposure, and female rats gaining less weight on the high-fat diet respective of exposure. Male rats exposed to nano-TiO₂ *in utero* had reduced ejection fraction prior to diet when compared to air controls. Female rats subjected to *in utero* nano-TiO₂ exposure showed a significant decrease in cardiac output following 12 weeks of high-fat diet. Development of cardiovascular impairments and ultimately cardiac dysfunction and disease following *in utero* exposures highlights the need for occupational and environmental monitoring of nanoparticulate exposure.

Keywords Pregnancy · Cardiac · Nanomaterial · Diet · Sexually dimorphic

Introduction

Critical windows during fetal development, such as organogenesis, are highly susceptible to environmental insults that can lead to failed organ development, teratogenesis, or even death. A properly functioning mammalian placenta serves a protective barrier during gestation as it selectively allows certain nutrients and other molecules to pass between maternal and fetal circulation, while impeding other molecules, toxicants, or pathogens from entering the fetal circulation. However, in the case of improper placentation or placental damage, harmful elements from the maternal circulation may impinge upon fetal development. Engineered

nanomaterials (ENM) are one such toxicant that have been shown to cross the placenta and into the fetus. Multiwall carbon nanotubes [1, 2], fullerenes [3], and nano-titanium dioxide (nano-TiO₂) [4, 5] have all been shown to accumulate in fetal tissues. Nano-TiO₂ is used across a wide range of commercial applications from a food colorant to ultraviolet light protection in cosmetics [6, 7]. Due to the accelerated use and ubiquitous nature of nano-TiO₂ exposure, reproductive studies on the impacts of ENM during gestation are critical for determining risks toward fetomaternal health and regulatory or clinical guidelines.

Gestational nano-TiO₂ exposure has been shown to alter maternal gut microbiota [8], neonatal body weight [9], neonatal pulmonary development [10], and fetal-to-young adult cardiac function [11] in rodents. Nano-TiO₂ accumulates in human and rodent cardiac tissue [12–14], and nano-TiO₂ particles are internalized by rat cardiomyoblasts *in vitro*, impacting cell viability, proliferation, and mitochondrial function [15]. Oral nano-TiO₂ exposure reduces levels of cellular cytochrome C (Cyt-C), increases apoptosis and collagen depositions in rat cardiac tissue

✉ Elizabeth Bowdridge
ebowdrid@hsc.wvu.edu

¹ Department of Physiology, Pharmacology, and Toxicology, West Virginia University, Morgantown, WV 26505, USA

² Mitochondria, Metabolism & Bioenergetics Working Group, West Virginia University School of Medicine, Morgantown, WV, USA

[16]. Furthermore, chronic nano-TiO₂ exposure decreases systolic and diastolic blood pressure in rats, with onset of cardiac changes appearing earlier in female rats when compared to males [17].

Following phagocytosis, nano-TiO₂ particles can bind to the mitochondrial membrane, disrupting the electron transport chain and generating oxides within the cell [18]. Prolonged permeabilization of the mitochondrial membrane activates cellular apoptotic and necrotic pathways, ultimately leading to cell death [19]. In addition to the induction of oxidant production, nano-TiO₂ severely inhibits the activity of several antioxidant enzymes such as superoxide dismutase (SOD), catalase (CAT), glutathione peroxidase (GSH-Px), and glutathione (GSH) [20]. While most commonly studied for damaging effects to the liver, nano-TiO₂ is a ubiquitous toxicant that has been shown to cause damage in the heart, brain, kidneys, and reproductive systems [21].

Although gestational nano-TiO₂ exposure is known to cross into the fetoplacental unit [22] and exert toxic effects on the heart [11], brain [23], liver [24], and transcriptome [25] of the progeny, adult health deficits resulting from *in utero* exposure have only been studied sparingly. It has been shown in a rat model that *in utero* ENM exposure may lead to the development of coronary artery disease and morphological changes in the heart independent of inflammatory and lipidomic changes [26]. Given the substantial impact of placental function on the fetal heart and development of congenital heart defects [27], the current study seeks to ascertain lasting cardiac and metabolic effects of *in utero* nano-TiO₂ exposure, in combination

with a high-fat diet, which serves as a second insult in adulthood (Table 1).

Materials and Methods

Animal Model

Female, Sprague–Dawley (SD rats) were purchased from Hilltop Laboratories (Scottsdale, PA), and housed in an Assessment and Accreditation of Laboratory Animal Care (AAALAC) approved facility at West Virginia University (WVU) under a regulated temperature and 12:12 h light–dark cycle. Rats ($n=6$ per group) were randomly assigned to sham-control or nano-TiO₂ exposure groups and acclimated for 48–72-h before mating. Rats had *ad libitum* access to food and water throughout the acclimation period. Vaginal smears were used to confirm estrus prior to pairing, and pregnancy was confirmed via presence of a seminal plug. To increase the likelihood of viable progeny, pregnant rats were exposed to nano-TiO₂ aerosols as described below after implantation on gestational day 10 (GD 10), as prior indications of inhalation exposure results in near to total loss of pregnancy [22]. Weights of pregnant dams were recorded weekly. Dams were allowed to deliver pups naturally, and dam characteristics can be found in Table 2. Pups were housed with dams postnatally and weaned based on sex on postnatal day 21. Weight-matched pups from typical litters were selected for subsequent analysis. Litters of <5 were omitted as atypical as offspring are significantly larger. A total of 32 ($n=8$ per group) animals were selected and divided evenly into the 4 filtered air groups, while 48 animals ($n=12$ per group) were divided evenly among the nano-TiO₂ exposed group. At 12 weeks of age animals were randomly assigned respective groups were placed on high-fat diets (Fig. 1). Animal received either a grain-based diet (T2918, Teklad INC ®), or the D12492 rodent diet with 60 kcal% fat (high-fat diet/HFD; Research Diets INC ®; Table 1). Complete formulations including micro-nutrient vales can be found in Supplemental Table 1. The HFD was refreshed every 2–3 days to limit oxidation and prevent spoiling. Animals continued to be weighed weekly for 8 weeks; at which time a subsequent echocardiographic assessment were conducted at 20 weeks of age. Animals

Table 1 Macronutrient compositions of dietary conditions used in study

	Grain-Based Diet	High-Fat Diet
Cat. number	2918	D12492
Protein	18.40%	26.20%
Fiber	3.80%	6.50%
Carbohydrates	44.20%	25.60%
Fat	6%	34.90%

Values expressed as percent of total composition for diets

Table 2 Maternal Litter characteristics for each exposure condition

Dam Characteristics				
Exposure	Number of Litters (N)	Weight (g) GD Day 19	Litter size	Sex ratio Male: Female
Sham-Control	5	333 ± 16.71	10 ± 1.04	0.440.55 ± 0.06
Nano-TiO ₂ Exposed	6	319 ± 15.09	13 ± 1.34	0.46:0.53 ± 0.04

Data provided as mean ± standard error

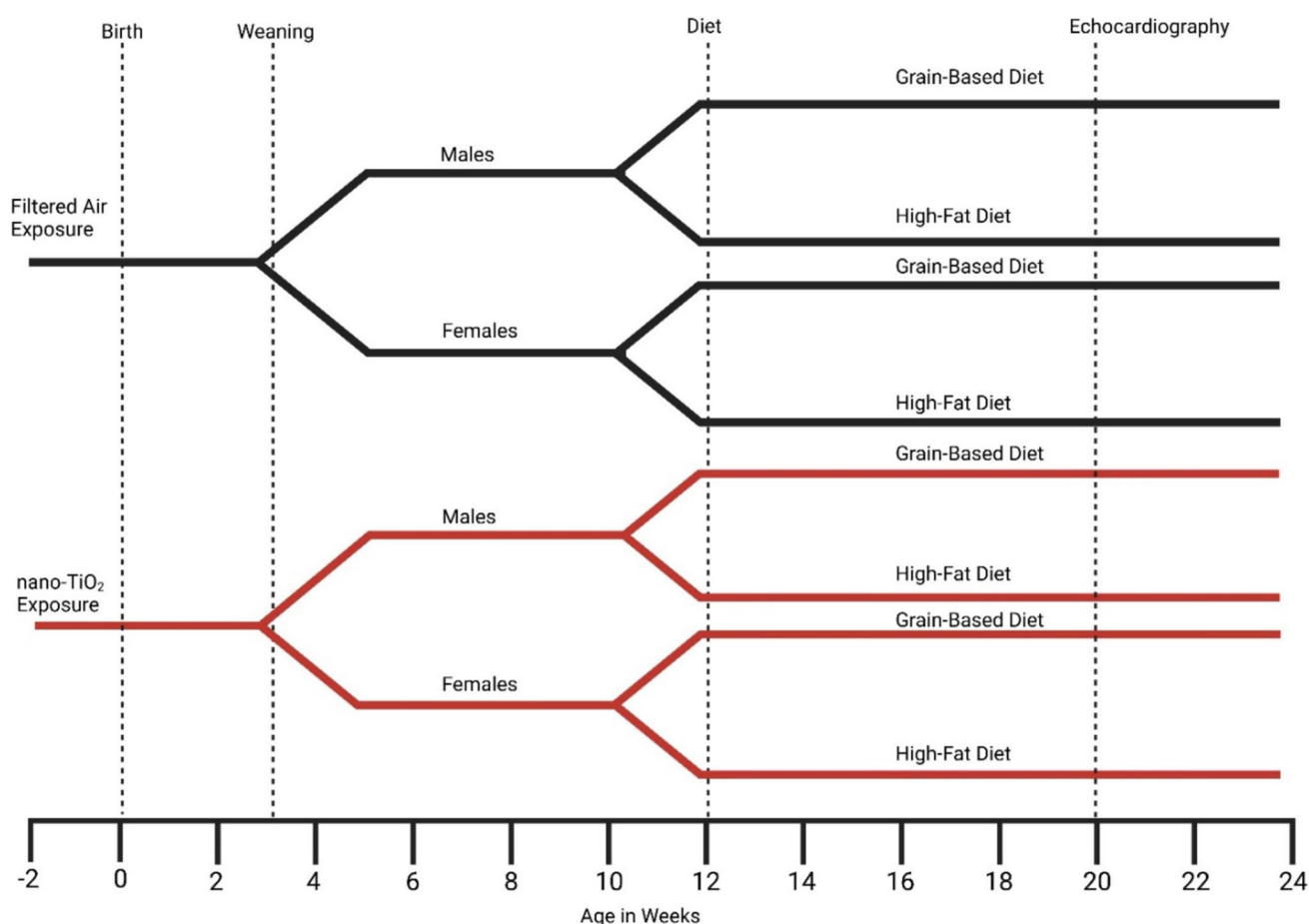


Fig. 1 Schematic detailing the study timeline of *in utero* exposures, dietary treatments, and cardiac and metabolic endpoints

continued on the diet for four additional weeks before final weights were taken and animals were euthanized. All procedures were approved by the Institutional Animal Care and Use Committee of West Virginia University.

Engineered Nanomaterial

Nano-TiO₂ powder was obtained from Evonik (Aeroxide TiO₂, Parsippany, NJ). It is a mixture composed of anatase (80%) and rutile (20%) TiO₂. Particle characteristics have been determined including the primary particle size (21 nm), the specific surface area (48.08 m/g), and the Zeta potential (-56.6 mV) [7].

Aerosol size distributions were determined in the exposure chamber while the target mass concentration was being maintained at 12 ± 0.13 mg/m³ with: (1) a high-resolution electrical low-pressure impactor (ELPI+; Dekati, Tampere, Finland), (2) a scanning particle mobility sizer (SMPS 3938; TSI Inc., St. Paul, MN), and (3) an aerodynamic particle sizer (APS 3321; TSI Inc., St. Paul, MN), and a Nano

Micro-Orifice Uniform Deposit Impactor (MOUDI 115R, MSP Corp, Shoreview, MN).

Inhalation Exposure

Nano-TiO₂ aerosols were generated using a high-pressure acoustical generator (HPAG, IESTechno, Morgantown, WV). The output of the generator was fed into a Venturi pump (JS-60 M, Vaccon, Medway, MA) which further de-agglomerated the particles. The nano-TiO₂ aerosol/air mix then entered the whole-body exposure chamber. A personal DataRAM (pDR-1500; Thermo Environmental Instruments Inc., Franklin, MA) was utilized to sample the exposure chamber air to determine the aerosol mass concentration in real-time. Feedback loops within the software automatically adjusted the acoustic energy to maintain a stable mass concentration during the exposure. Gravimetric measurements were conducted on Teflon filters concurrently with the DataRAM measurements to obtain a calibration factor. The gravimetric measurements were also conducted during each exposure to calculate the mass concentration measurements reported in

the study. Bedding material soaked with water was used in the exposure chamber to maintain humidity (30–70%) during exposures. Sham-control animals were exposed to HEPA filtered air only (25 mL/min) with similar temperature and humidity chamber conditions.

Inhalation exposures in F0 dams lasted for 6 non-consecutive days after GD 10 to decrease animal stress and problems with implantation. Exposures began on GD 12 and lasted until GD19. The pregnant rats were exposed to an average target concentration of 12 mg/m³. While trace amounts of TiO₂ may be ingested with grooming following exposures, there was no direct exposure of TiO₂ to the offspring after birth for the duration of the study. This concentration of 12 mg/m³ was chosen to match our previous late gestation inhalation exposure studies [14, 15]. To estimate lung dose with nano-TiO₂ aerosols [13] we used the equation: $D = F \cdot V \cdot C \cdot T$, where F is the deposition fraction (10%), V is the minute ventilation (208.3 cc), C equals the mass concentration (mg/m³), and T equals the exposure duration (minutes) [67]. This exposure paradigm (12 mg/m³, 6 h/exposure, 6 days) produced an estimated target lung dose of $525 \pm 16 \mu\text{g}$ with the last exposure conducted 24 h prior to sacrifice and experimentation. These calculations represent total lung deposition and do not account for clearance (MPPD Software v 2.11, Arlington, VA).

Echocardiography M-Mode, and Doppler Imaging

At 20 weeks of age, the F1 Sprague–Dawley offspring of the F0 dams exposed to nano-TiO₂ or filtered air were taken for echocardiography. Prior to imaging, animals were anesthetized via isoflurane (2.5–3%) adjusted to maintain a steady heartrate, and a depilatory cream was used to remove excess hair from the chest. Ultrasound images were taken using the Vevo F2 Imaging System (Visual Sonics, Toronto, Canada). Briefly, M-mode measurements were taken along the short-axis plane to determine the LV thickness (interventricular septal, inner, and posterior wall) were conducted on adjacent end-systolic and end-diastolic peaks in relation to LV trace analysis. All ultrasound procedures were carried out by one imaging specialist, taken at a frame rate of 109–284 frames/s. M-mode and Doppler echocardiography were examined using averaged values from at least three replicate analyses from each animal. All measures were completed by one analyst blinded to exposure groups.

Tissue Collection

At the conclusion of the study, animals were anesthetized via isoflurane (5%) and euthanized via exsanguination. Cardiac tissue was then immediately removed and rinsed in ice-cold phosphate buffered saline to remove excess blood before being processed for mitochondrial extraction. Other organs

were excised, weighed, and flash-frozen for independent studies.

Mitochondrial Function Assays

ETC Complex activities (I, II, III, IV, and V) were measured in hearts of adult offspring as previously described [28]. Left and right ventricular tissue was homogenized using the Polyttron PowerGen 500 S1 tissue homogenizer (Fisher Scientific, Hampton, NH) in NP-40 buffer (20 mM Tris, 137 mM NaCl, 10% Glycerol, 1% Triton X-100, 2 mM EDTA) [29]. Samples were centrifuged for 10 min at 10 000 xg (4 °C) and the supernatant was used for the activity assays. The protein homogenates were used to measure activities of ETC complexes I, II, III, IV, and V (ATP synthase). ETC complex I and III activities were determined by measuring the reduction of decylubiquinone (I) and cytochrome c (III) in cardiac protein lysate of adult offspring. ETC complex II activity was measured using the reduction of dichlorophenolindophenol. ETC complex IV activity was determined by measuring the oxidation of reduced cytochrome c, while complex V activity was determined by measuring oligomycin-sensitive ATPase activity through pyruvate kinase and phosphoenolpyruvate in cardiac protein lysate of adult offspring. The Molecular Devices Flex Station 3 Multi-Mode microplate reader (Sunnyvale, CA) was used to measure all assays spectrophotometrically. Protein content was normalized using the Bradford method, with bovine serum albumin protein assay standards. Final values were expressed as Unit/nanogram (I–IV) or milligram (V) of protein, where Unit = nanomoles of substrate oxidized (minute^{−1}).

Statistical Analysis

Weight gain was analyzed using two-way analysis of variance (ANOVA) with repeated measures. All other physiological characteristics were assessed by two-way mixed-effects ANOVA. If statistical significance occurred, then a Tukey post hoc test was used for all ANOVA analysis. All data are reported as mean \pm SEM, unless otherwise stated. Significance was set at $p \leq 0.05$. All data was analyzed in GraphPad Prism 10.

Results

Animal Weights

Animals were weighed weekly starting at 6 weeks of age to measure changes in weight gain. At 6 weeks of age, both males (106 ± 1.8) and females (94 ± 2.9) receiving *in utero* exposure to nano-TiO₂ weighed significantly less than filtered air controls (137 ± 3.2 ; 116 ± 1.4 , respectively (Fig. 2A).

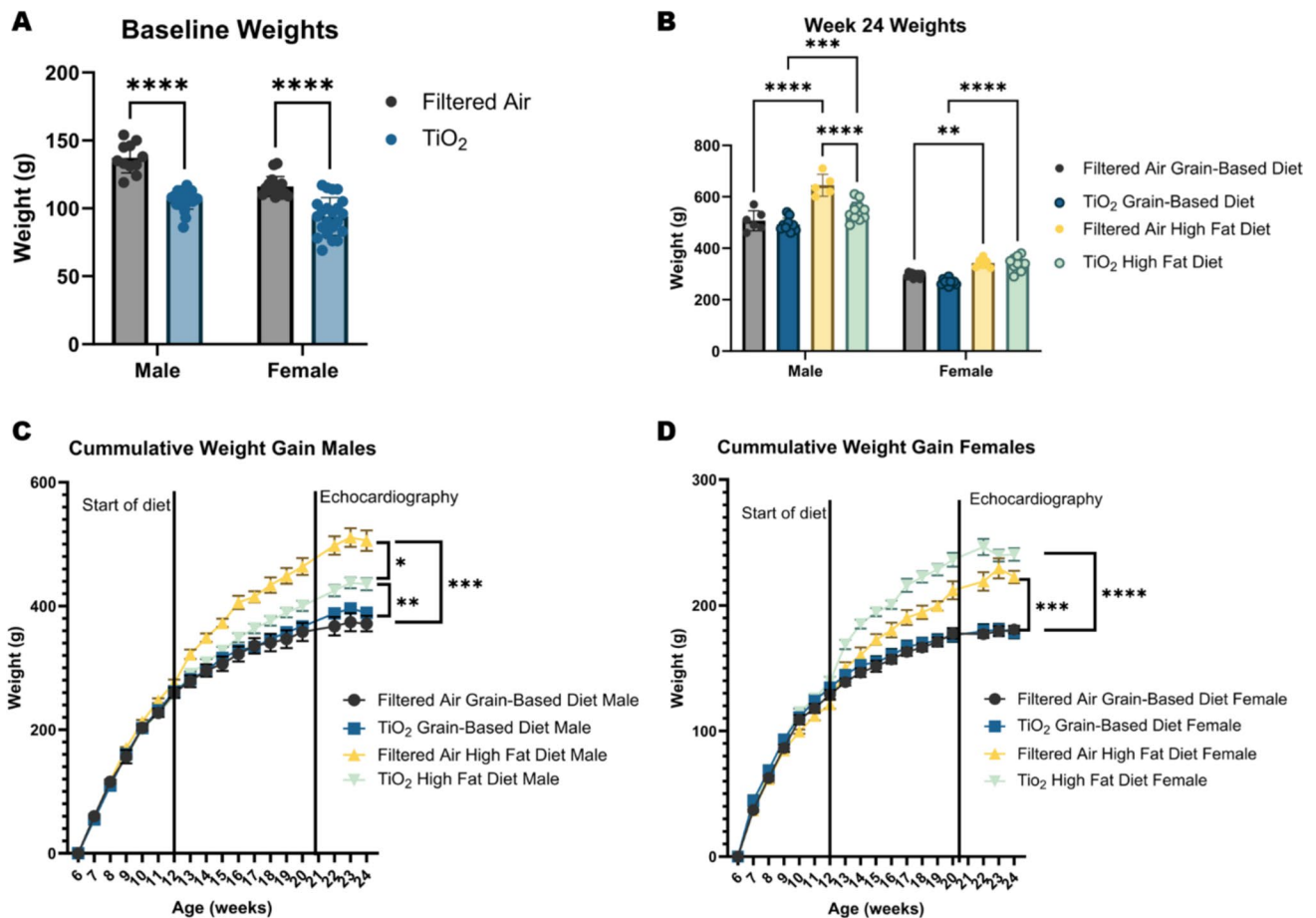


Fig. 2 **A** Baseline animal weights at 6 weeks of age between exposures. **B** Animal weights at 24 weeks of age. **C, D** Cumulative weight gain over the course of the study for male and female animals, respec-

tively. Asterisks show significance ($p < 0.05$) by 2-Way ANOVA (**A** and **B**), or by 2-way repeated measures ANOVA (**C** and **D**)

Males maintained on the GBD grew to 506 ± 16.0 g in the air control and 492 ± 8.0 g in the nano-TiO₂ group. Males given the HFD showed significant increases in weight gain to 645 ± 18.9 g in the air control, and 544 ± 10.2 g in the nano-TiO₂ exposed group. Females on the GBD grew to 295 ± 3.2 g in the air control and 268 ± 3.6 g in the nano-TiO₂ exposed group. Females on the HFD also showed significant increases in growth, weighing 342 ± 7.3 g in the air control and 338 ± 8.2 g in the nano-TiO₂ exposed group (Fig. 2B).

Heart Function

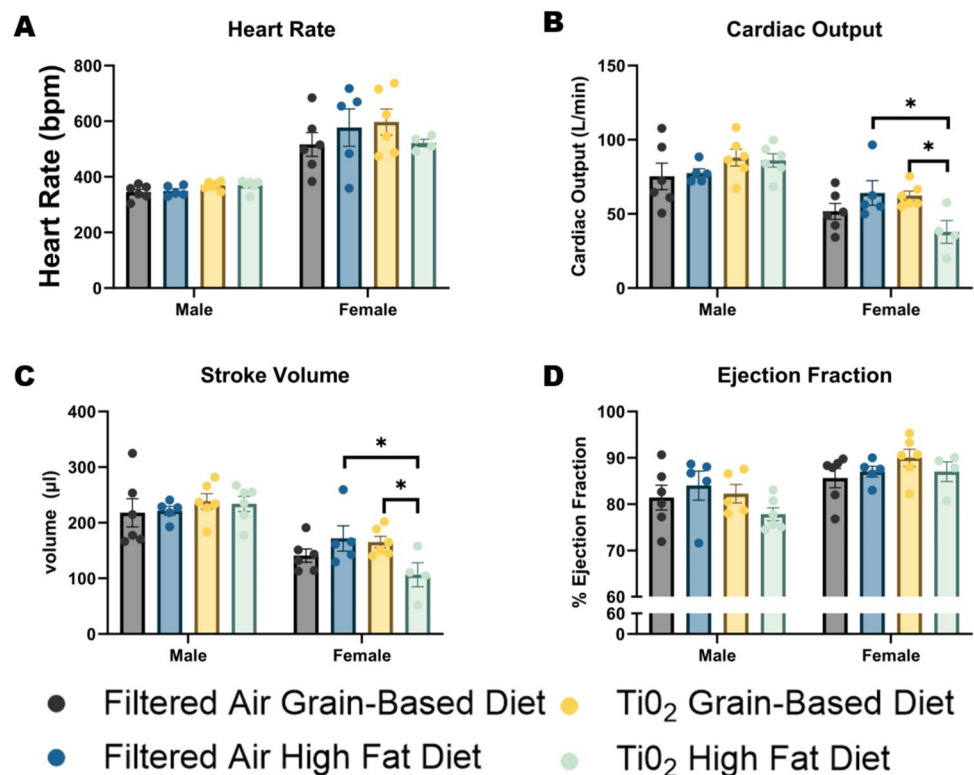
Echocardiography was performed at 20 weeks of age, following 8 weeks on respective diets. F1 females presented with higher heartrate across all exposure groups when compared to males counterparts (Fig. 3A). F1 males receiving *in utero* exposure to nano-TiO₂ presented with higher overall heartrate compared to filtered air controls, with no significant difference by diet. Female exposed to nano-TiO₂ in

utero presented with significant decreases in cardiac output and stroke volume compared to filtered air control females (Fig. 3B, C). Additionally, F1 exposed females has significantly decreased diastolic diameter and volume when compared to filtered air controls. Both sexes showed significant changes in left ventricular posterior wall (LVPW) thickness during diastole due to diet. Data from both sexes are summarized in Table 3.

Mitochondrial Function

Heart tissue homogenate was used to isolate cardiac mitochondrial fractions from each group. Males receiving the grain-based diet showed a significant reduction in Complex I activity due to *in utero* nano-TiO₂ exposure compared to filtered air controls. In contrast, females exhibited a significant increase in Complex I activity as a result of exposure in both dietary groups. Additionally, HFD females had significantly increased Complex I activity compared to the grain-based diet group among filtered air *in utero* exposure (Fig. 4A).

Fig. 3 Echocardiography of F1 male and female hearts at 20 weeks of age after 8 weeks of diet treatment. **A** Heart rate. **B** Cardiac output **C** Stroke volume, **D** Ejection fraction. Asterisks show significance ($p < 0.05$) by 2-Way ANOVA



Males in the nano-TiO₂ grain-based diet group had a significant reduction in Complex II activity, with no significant changes in Complex II activity observed in males on the HFD or females across all groups (Fig. 4B). Males in the nano-TiO₂ HFD group had significantly increased Complex III activity compared to filtered air controls on the same diet. No significant changes were observed in Complex III activity in males on the grain-based diet or female animals between all groups (Fig. 4C). Filtered air HFD males showed a significant reduction in Complex IV activity when compared to grain-based diet controls, a similar although non-significant reduction was also observed in nano-TiO₂ males (Fig. 4D). There was no observed change in Complex IV activity in females between all groups (Fig. 4D). Male animals showed no difference in Complex V activity between all groups, while there was a trend for reduced Complex V activity in nano-TiO₂ grain-based diet females compared to filtered air controls ($p = 0.076$).

Discussion

Similar to previous studies [22, 30], *in utero* nano-TiO₂ exposure resulted in decreased pup weight that persisted 6 weeks after birth. Risks for low birth weight following maternal inhalation of air pollution and specifically particulate matter are well documented [31–33]. Recent studies characterizing impacts of specific elements of airborne fine

particulate matter found increases in titanium (Ti) within particulate matter to be associated with a 12% increased risk of low birth weight [34]. The present study found a sexually dimorphic response to weight gain between animals exposed to nano-TiO₂ *in utero*. Exposed males gained significantly less weight on a HFD compared to air controls, whereas exposure did not significantly affect cumulative weight gain in females. Though it has been reported that intraperitoneal injection of nano-TiO₂ may cause loss of appetite in mice [35], it is unclear to what extent the *in utero* exposure may alter nutritional regulation into adulthood. Given that both sexes receiving nano-TiO₂ exposure *in utero* had persistently lower body weight throughout sexual maturity (Fig. 2A), it seems unlikely the sex-specific response to HFD was compensatory from a nutritional standpoint, and more likely driven by differences in endocrine or neural signaling. The current study utilized a commercially available dietary formulation for our HFD groups. Differences in macronutrient and micronutrient diversity between the two groups may have significant metabolic impacts. Though the described study lacked the statistical number necessary to incorporate an ingredient-matched control group, future studies may benefit from exploring more refined metabolic adjustment of *in utero* exposed offspring during development. Previously, our laboratory has shown endocrine disruption, specifically estradiol, in directly exposed dams and F1 female offspring during gestation [30]. Additionally, *in utero* exposure also results in significant impairment in cognitive behaviors in

Table 3 Cardiac parameters by echocardiography taken at 20 weeks of age

Parameter	Male				Female			
	Source of Variation	% of total variation	<i>P</i> value	Summary	Source of Variation	% of total variation	<i>P</i> value	Summary
Heart rate	Interaction	0.1345	0.8541	ns	Interaction	9.899	0.1868	ns
	Exposure	25.42	0.0191	*	Exposure	0.3457	0.8002	ns
	Diet	0.3221	0.7762	ns	Diet	0.1163	0.8832	ns
Diameter;Systole	Interaction	1.308	0.6025	ns	Interaction	1.419	0.6014	ns
	Exposure	10.33	0.1531	ns	Exposure	14.47	0.1073	ns
	Diet	0.2695	0.8126	ns	Diet	0.02518	0.9443	ns
Diameter;Diastole	Interaction	0.00008085	0.999	ns	Interaction	25.11	0.0214	*
	Exposure	8.028	0.2132	ns	Exposure	9.761	0.1325	ns
	Diet	0.04192	0.9268	ns	Diet	4.297	0.3092	ns
Volume;Systole	Interaction	0.9174	0.6674	ns	Interaction	0.8814	0.6853	ns
	Exposure	6.893	0.2463	ns	Exposure	11.61	0.1529	ns
	Diet	1.235	0.6184	ns	Diet	0.1758	0.8561	ns
Volume;Diastole	Interaction	0.02018	0.9496	ns	Interaction	23.58	0.0287	*
	Exposure	6.506	0.264	ns	Exposure	8.566	0.168	ns
	Diet	0.3266	0.7993	ns	Diet	2.367	0.4594	ns
Stroke Volume	Interaction	0.2793	0.8158	ns	Interaction	29.2	0.0141	*
	Exposure	4.547	0.3524	ns	Exposure	6.059	0.23	ns
	Diet	0.003658	0.9787	ns	Diet	2.816	0.4078	ns
Ejection Fraction	Interaction	10.07	0.1565	ns	Interaction	6.617	0.2623	ns
	Exposure	5.865	0.2739	ns	Exposure	6.555	0.2645	ns
	Diet	0.7323	0.6947	ns	Diet	0.8344	0.6857	ns
Cardiac Output	Interaction	0.483	0.7471	ns	Interaction	32.89	0.0082	**
	Exposure	13.51	0.0996	ns	Exposure	5.933	0.2212	ns
	Diet	0.003228	0.9789	ns	Diet	3.483	0.3442	ns
LVAW; Systole	Interaction	0.8895	0.6753	ns	Interaction	4.881	0.3569	ns
	Exposure	4.925	0.3293	ns	Exposure	1.59	0.5959	ns
	Diet	1.314	0.611	ns	Diet	0.007306	0.9712	ns
LVAW; Diastole	Interaction	0.06277	0.9113	ns	Interaction	3.791	0.3369	ns
	Exposure	4.178	0.3685	ns	Exposure	12	0.0966	ns
	Diet	1.924	0.5393	ns	Diet	22.53	0.0276	*
LVPW; Systole	Interaction	5.436	0.2499	ns	Interaction	1.916	0.493	ns
	Exposure	0.04973	0.9108	ns	Exposure	19.21	0.0404	*
	Diet	22.22	0.0268	*	Diet	11.2	0.1086	ns
LVPW; Diastole	Interaction	1.545	0.5144	ns	Interaction	0.6001	0.7086	ns
	Exposure	0.7396	0.651	ns	Exposure	10.4	0.1321	ns
	Diet	32.23	0.0068	**	Diet	20.71	0.0393	*

Asterisks show significance ($p < 0.05$) by 2-Way ANOVA

adult F1 males [23]. Taken together, these studies show sexually dimorphic endocrine and neuronal responses of rats into adulthood and may contribute to the differences in weight gain between males and females observed herein.

Obesity is a known risk factor for the development of cardiovascular disease (CVD; [36]). Given the low birthweight previously seen due to ENM exposure [37], along with the persistent low post pubertal weight in exposed offspring and weight gain observed in this study, we investigated potential

deficits in cardiac function. Echocardiographic assessment found few differences in overall heart function for males following 8 weeks of HFD. Females showed more robust alterations in cardiac function, where *in utero* nano-TiO₂ exposed rats presented with significantly lower cardiac output than both *in utero* exposed animals on grain-based diet and filtered air controls on HFD. CVD remains the leading cause of mortality for both men and women in the United States and worldwide [38]. Despite similar rates in overall

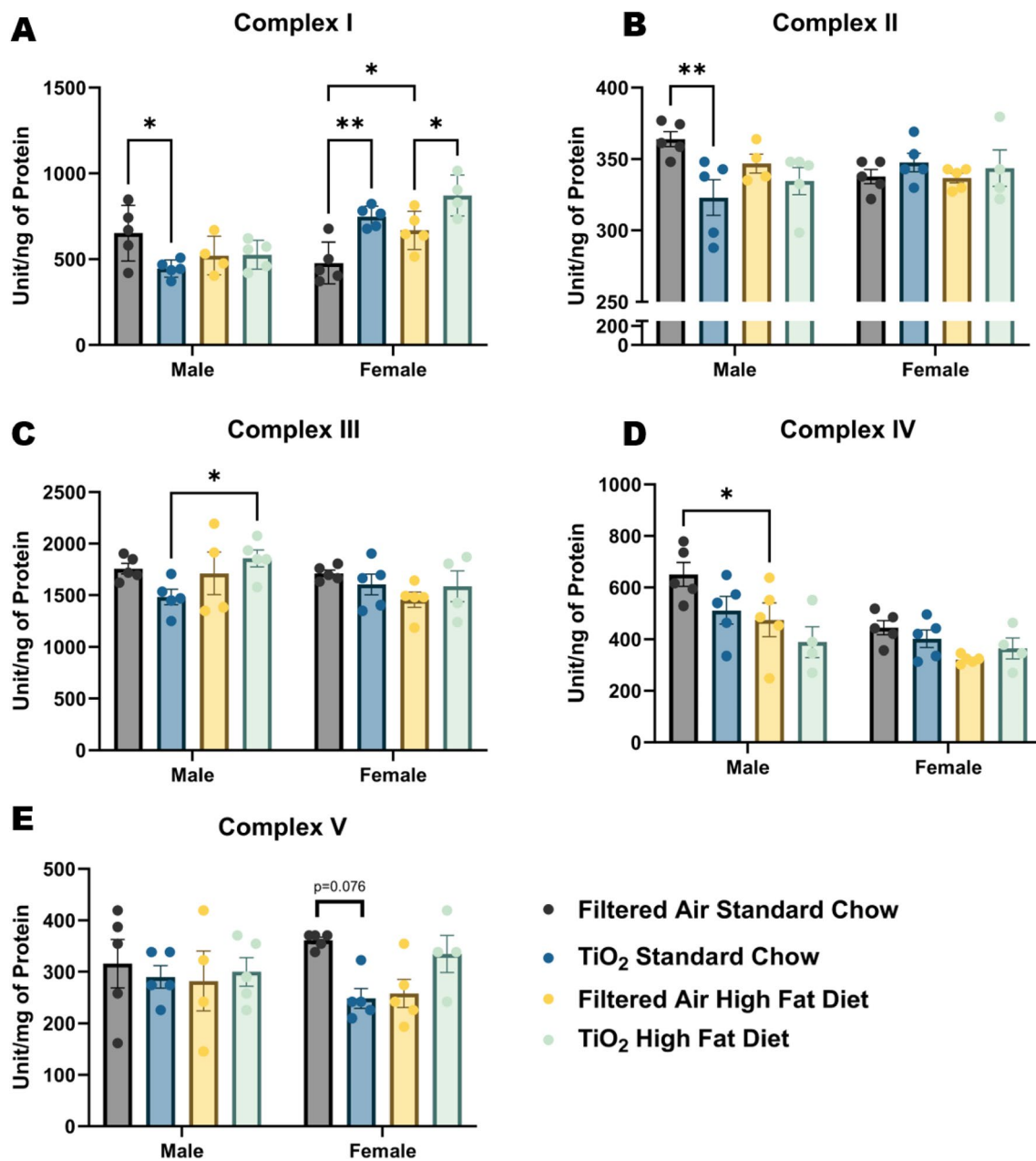


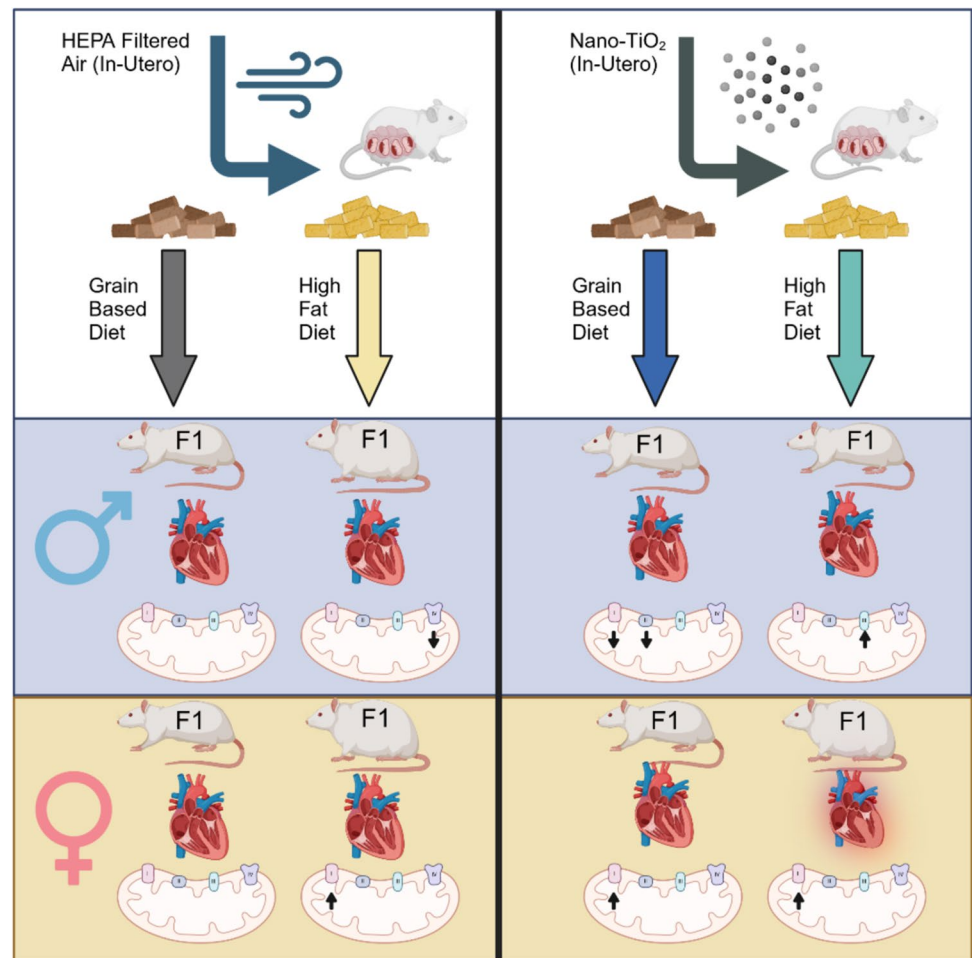
Fig. 4 Cardiac mitochondrial function assessment across all complexes. Asterisks show significance ($p < 0.05$) by 2-Way ANOVA

mortality, the prevalence of CVD is higher in males, with an earlier onset. Men and women share several common risk factors for CVD, including diabetes, hypertension, and smoking, while there are several female-specific risk factors such as menopause, polycystic ovary syndrome, and adverse pregnancy outcomes [39]. The reduced cardiac output in the female HFD animals receiving the *in utero* nano-TiO₂ exposure was of particular interest given the accompanying mitochondrial changes. Given these data, further investigation into cardiac stress and the role of endocrine signaling for cardioprotective effects may be insightful. This current

study utilized a relatively short timeframe to examine cardiovascular changes, where future research may benefit from more long-term analysis of the development of cardiac dysfunction.

Male cardiac mitochondria had decreased function in complexes 1–4 across the exposure and dietary conditions when compared to air controls on the grain-based diet. Female cardiac mitochondria exhibited a pronounced exposure-driven increase in Complex I (NADH: ubiquinone oxidoreductase) activity. Complex I has high capacity for the generation of reactive oxygen species (ROS; [40]),

Fig. 5 Graphical summary of sex-specific effects of diet and exposure



being able to produce both superoxide (predominantly) as well as hydrogen peroxide [41]. Previous reports on rats exposed to nano-TiO₂ *in utero* showed that young adult rats (6–12 weeks) presented with decreased Complex I activity [11]. Mitochondria in female ventricular cardiomyocytes have been shown to exhibit higher incorporation of subunits into supercomplexes, limiting mito-ROS production when compared to males [42]. At the onset of exposure (GD 10), fetal cardiac myocytes are considered “very immature,” gradually increasing in complexity and metabolic capability. The metabolic shift from glycolysis (predominantly oxidative phosphorylation) does not fully transition until approximately 3 weeks postnatally [43]. One potential explanation for functional differences in mitochondrial activity is cardiac distribution. Male cardiac mitochondria in mice have been reported to be both moderately less abundant, as well as morphologically impaired (fragmented, shorter in size) when compared to matched female cardiac mitochondria [44]. The standardization methods for the mitochondrial activity assays may be unable to account for these sex differences. The potential effects of nano-TiO₂ to produce ROS-driven mitochondrial dysfunction in fetal cardiomyocytes

remains understudied, and lasting effects on mitochondria of adult cardiomyocytes also needs to be studied further for impacts on cardiac health.

Altogether, data collected within this study present clear sexually dimorphic responses in offspring weight gain and cardiac function due to *in utero* exposure and/or dietary treatment in adulthood. Female rats had significant exposure-driven increases in mitochondrial Complex I activity, and F1 female rats receiving nano-TiO₂ and HFD had significantly reduced cardiac output (Fig. 5). In contrast, male rats showed reduced weight gain on the HFD, independent of changes in cardiac function. Future studies should investigate the underlying mechanism(s) conferring these sexually dimorphic changes, including endocrine disruption, epigenetic modifications, and changes in orexigenic and anorexigenic neural populations.

Supplementary Information The online version contains supplementary material available at <https://doi.org/10.1007/s12012-025-09960-y>.

Author Contribution R.H. and E.B. wrote main manuscript text and prepared Figs. 1, 2, 3 and 4. T.G., R. N., and V. N. assisted with experimental design and data analysis, R. N prepared Fig. 5. E.M. performed

experimental procedures and wrote methods for Fig. 4. All authors reviewed the manuscript.

Funding This study was funded National Institute for Occupational Safety and Health, 5K01OH012320-03.

Data Availability No datasets were generated or analyzed during the current study.

Declarations

Competing Interests The authors declare no competing interests.

Open Access This article is licensed under a Creative Commons Attribution-NonCommercial-NoDerivatives 4.0 International License, which permits any non-commercial use, sharing, distribution and reproduction in any medium or format, as long as you give appropriate credit to the original author(s) and the source, provide a link to the Creative Commons licence, and indicate if you modified the licensed material. You do not have permission under this licence to share adapted material derived from this article or parts of it. The images or other third party material in this article are included in the article's Creative Commons licence, unless indicated otherwise in a credit line to the material. If material is not included in the article's Creative Commons licence and your intended use is not permitted by statutory regulation or exceeds the permitted use, you will need to obtain permission directly from the copyright holder. To view a copy of this licence, visit <http://creativecommons.org/licenses/by-nc-nd/4.0/>.

References

- Qi, W., Bi, J., Zhang, X., Wang, J., Wang, J., Liu, P., Li, Z., & Wu, W. (2014). Damaging effects of multi-walled carbon nanotubes on pregnant mice with different pregnancy times. *Science and Reports*, 4, 4352.
- Huang, X., Zhang, F., Sun, X., Choi, K. Y., Niu, G., Zhang, G., Guo, J., Lee, S., & Chen, X. (2014). The genotype-dependent influence of functionalized multiwalled carbon nanotubes on fetal development. *Biomaterials*, 35, 856–865.
- Snyder, R. W., Fennell, T. R., Wingard, C. J., Mortensen, N. P., Holland, N. A., Shannahan, J. H., Pathmasiri, W., Lewin, A. H., & Sumner, S. C. (2015). Distribution and biomarker of carbon-14 labeled fullerene C60 ([14C(U)]C60) in pregnant and lactating rats and their offspring after maternal intravenous exposure. *Journal of Applied Toxicology*, 35, 1438–1451.
- D'Errico, J. N., Doherty, C., Reyes George, J. J., Buckley, B., & Stapleton, P. A. (2022). Maternal, placental, and fetal distribution of titanium after repeated titanium dioxide nanoparticle inhalation through pregnancy. *Placenta*, 121, 99–108.
- Lee, J., Jeong, J. S., Kim, S. Y., Park, M. K., Choi, S. D., Kim, U. J., Park, K., Jeong, E. J., Nam, S. Y., & Yu, W. J. (2019). Titanium dioxide nanoparticles oral exposure to pregnant rats and its distribution. *Particle and Fibre Toxicology*, 16(1), 31.
- Fage, S. W., Muris, J., Jakobsen, S. S., & Thyssen, J. P. (2016). Titanium: A review on exposure, release, penetration, allergy, epidemiology, and clinical reactivity. *Contact Dermatitis*, 74(6), 323–345.
- Wiesenthal, A., Hunter, L., Wang, S., Wickliffe, J., & Wilkerson, M. (2011). Nanoparticles: Small and mighty. *International Journal of Dermatology*, 50(3), 247–254.
- Mao, Z., Li, Y., Dong, T., Zhang, L., Zhang, Y., Li, S., Hu, H., Sun, C., & Xia, Y. (2019). Exposure to titanium dioxide nanoparticles during pregnancy changed maternal gut microbiota and increased blood glucose of rat. *Nanoscale Research Letters*, 14(1), 26.
- Li, X., Luo, Y., Ji, D., Zhang, Z., Luo, S., Ma, Y., Cao, W., Cao, C., Saw, P. E., Chen, H., & Wei, Y. (2023). Maternal exposure to nano-titanium dioxide impedes fetal development via endothelial-to-mesenchymal transition in the placental labyrinth in mice. *Particle and Fibre Toxicology*, 20(1), 48.
- Colnot, E., Cardoit, L., Cabirol, M. J., Roudier, L., Delville, M. H., Fayoux, A., Thoby-Brisson, M., Juvin, L., & Morin, D. (2022). Chronic maternal exposure to titanium dioxide nanoparticles alters breathing in newborn offspring. *Particle and Fibre Toxicology*, 19(1), 57.
- Hathaway, Q. A., Nichols, C. E., Shepherd, D. L., Stapleton, P. A., McLaughlin, S. L., Stricker, J. C., Rellick, S. L., Pinti, M. V., Abukabda, A. B., McBride, C. R., & Yi, J. (2017). Maternal-engineered nanomaterial exposure disrupts progeny cardiac function and bioenergetics. *American Journal of Physiology-Heart and Circulatory Physiology*, 312(3), H446–H458.
- Baranowska-Wojcik, E., Szwajgier, D., Oleszczuk, P., & Winarska-Mieczan, A. (2020). Effects of titanium dioxide nanoparticles exposure on human health-a review. *Biological Trace Element Research*, 193(1), 118–129.
- Husain, M., Wu, D., Saber, A. T., Decan, N., Jacobsen, N. R., Williams, A., Yauk, C. L., Wallin, H., Vogel, U., & Halapannavar, S. (2015). Intratracheally instilled titanium dioxide nanoparticles translocate to heart and liver and activate complement cascade in the heart of C57BL/6 mice. *Nanotoxicology*, 9, 1013–1022.
- Swiatkowska, I., Mosselmans, J. F. W., Geraki, T., Wyles, C. C., Maleszewski, J. J., Henckel, J., Sampson, B., Potter, D. B., Osman, I., Trousdale, R. T., & Hart, A. J. (2018). Synchrotron analysis of human organ tissue exposed to implant material. *Journal of Trace Elements in Medicine and Biology*, 46, 128–137.
- Colin-Val, Z., Vera-Márquez, C. D., Herrera-Rodríguez, M. A., del Pilar Ramos-Godínez, M., López-Saavedra, A., Cano-Martínez, A., Robledo-Cadena, D. X., Rodríguez-Enríquez, S., Correa, F., Delgado-Buenrostro, N. L., & Chirino, Y. I. (2022). Titanium dioxide (E171) induces toxicity in H9c2 rat cardiomyoblasts and Ex vivo rat hearts. *Cardiovascular Toxicology*, 22(8), 713–726.
- Herrera-Rodríguez, M. A., del Pilar Ramos-Godínez, M., Cano-Martínez, A., Segura, F. C., Ruiz-Ramírez, A., Pavón, N., Lira-Silva, E., Bautista-Pérez, R., Thomas, R. S., Delgado-Buenrostro, N. L., Chirino, Y. I., & López-Marure, R. (2023). Food-grade titanium dioxide and zinc oxide nanoparticles induce toxicity and cardiac damage after oral exposure in rats. *Particle and Fibre Toxicology*, 20(1), 43.
- Chen, Z., Wang, Y., Zhuo, L., Chen, S., Zhao, L., Luan, X., Wang, H., & Jia, G. (2015). Effect of titanium dioxide nanoparticles on the cardiovascular system after oral administration. *Toxicology Letters*, 239(2), 123–130.
- Hirakawa, K., Mori, M., Yoshida, M., Oikawa, S., & Kawanishi, S. (2004). Photo-irradiated titanium dioxide catalyzes site specific DNA damage via generation of hydrogen peroxide. *Free Radical Research*, 38(5), 439–447.
- Long, T. C., Saleh, N., Tilton, R. D., Lowry, G. V., & Veronesi, B. (2006). Titanium dioxide (P25) produces reactive oxygen species in immortalized brain microglia (BV2): Implications for nanoparticle neurotoxicity. *Environmental Science and Technology*, 40(14), 4346–4352.
- Cui, Y., Gong, X., Duan, Y., Li, N., Hu, R., Liu, H., Hong, M., Zhou, M., Wang, L., Wang, H., & Hong, F. (2010). Hepatocyte apoptosis and its molecular mechanisms in mice caused by titanium dioxide nanoparticles. *Journal of Hazardous Materials*, 183, 874–880.

21. Hong, J., & Zhang, Y. Q. (2016). Murine liver damage caused by exposure to nano-titanium dioxide. *Nanotechnology*, 27(11), 112001.
22. Stapleton, P. A., Minarchick, V. C., Yi, J., Engels, K., McBride, C. R., & Nurkiewicz, T. R. (2013). Maternal engineered nanomaterial exposure and fetal microvascular function: Does the Barker hypothesis apply? *American Journal of Obstetrics and Gynecology*, 209(3), 227 e221–211.
23. Engler-Chiurazzi, E. B., Stapleton, P. A., Stalnaker, J. J., Ren, X., Hu, H., Nurkiewicz, T. R., McBride, C. R., Yi, J., Engels, K., & Simpkins, J. W. (2016). Impacts of prenatal nanomaterial exposure on male adult Sprague-Dawley rat behavior and cognition. *Journal of Toxicology and Environmental Health. Part A*, 79(11), 447–452.
24. Naserzadeh, P., Ghanbary, F., Ashtari, P., Seydi, E., Ashtari, K., & Akbari, M. (2018). Biocompatibility assessment of titanium dioxide nanoparticles in mice fetoplacental unit. *Journal of Biomedical Materials Research. Part A*, 106(2), 580–589.
25. Stapleton, P. A., Hathaway, Q. A., Nichols, C. E., Abukabda, A. B., Pinti, M. V., Shepherd, D. L., McBride, C. R., Yi, J., Casttranova, V. C., Hollander, J. M., & Nurkiewicz, T. R. (2018). Maternal engineered nanomaterial inhalation during gestation alters the fetal transcriptome. *Particle and Fibre Toxicology*, 15, 1–15.
26. Fournier, S. B., Lam, V., Goedken, M. J., Fabris, L., & Stapleton, P. A. (2021). Development of coronary dysfunction in adult progeny after maternal engineered nanomaterial inhalation during gestation. *Science and Reports*, 11(1), 19374.
27. Camm, E. J., Botting, K. J., & Sferruzzi-Perri, A. N. (2018). Near to one's heart: The intimate relationship between the placenta and fetal heart. *Frontiers in Physiology*, 9, 629.
28. Kunovac, A., Hathaway, Q. A., Pinti, M. V., Durr, A. J., Taylor, A. D., Goldsmith, W. T., Garner, K. L., Nurkiewicz, T. R., & Hollander, J. M. (2021). Enhanced antioxidant capacity prevents epitranscriptomic and cardiac alterations in adult offspring gestationally-exposed to ENM. *Nanotoxicology*, 15(6), 812–831.
29. Hathaway, Q. A., Roth, S. M., Pinti, M. V., Sprando, D. C., Kunovac, A., Durr, A. J., Cook, C. C., Fink, G. K., Cheuvront, T. B., Grossman, J. H., Aljahli, G. A., Taylor, A. D., Giromini, A. P., Allen, J. L., & Hollander, J. M. (2019). Machine-learning to stratify diabetic patients using novel cardiac biomarkers and integrative genomics. *Cardiovascular Diabetology*, 18, 1–16.
30. Bowdridge, E. C., DeVallance, E., Garner, K. L., Griffith, J. A., Schafner, K., Seaman, M., Engels, K. J., Wix, K., Batchelor, T. P., Goldsmith, W. T., Hussain, S., & Nurkiewicz, T. R. (2022). Nano-titanium dioxide inhalation exposure during gestation drives redox dysregulation and vascular dysfunction across generations. *Particle and Fibre Toxicology*, 19(1), 18.
31. Bekkar, B., Pacheco, S., Basu, R., & DeNicola, N. (2020). Association of air pollution and heat exposure with preterm birth, low birth weight, and stillbirth in the US: A systematic review. *JAMA Network Open*, 3(6), e208243.
32. Liu, J., Chen, Y., Liu, D., Ye, F., Sun, Q., Huang, Q., Dong, J., Pei, T., He, Y., & Zhang, Q. (2023). Prenatal exposure to particulate matter and term low birth weight: Systematic review and meta-analysis. *Environmental Science and Pollution Research International*, 30(23), 63335–63346.
33. Steinle, S., Johnston, H. J., Loh, M., Mueller, W., Vardoulakis, S., Tantrakarnapa, K., & Cherrie, J. W. (2020). In utero exposure to particulate air pollution during pregnancy: Impact on birth weight and health through the life course. *International Journal of Environmental Research and Public Health*, 17(23), 8948.
34. Bell, M. L., Belanger, K., Ebisu, K., Gent, J. F., & Leaderer, B. P. (2012). Relationship between birth weight and exposure to airborne fine particulate potassium and titanium during gestation. *Environmental Research*, 117, 83–89.
35. Chen, J., Dong, X., Zhao, J., & Tang, G. (2009). In vivo acute toxicity of titanium dioxide nanoparticles to mice after intraperitoneal injection. *Journal of Applied Toxicology*, 29(4), 330–337.
36. Kruszewska, J., Cudnoch-Jedrzejewska, A., & Czarzasta, K. (2022). Remodeling and fibrosis of the cardiac muscle in the course of obesity-pathogenesis and involvement of the extracellular matrix. *International Journal of Molecular Sciences*, 23(8), 4195.
37. Griffith, J. A., Garner, K. L., Bowdridge, E. C., DeVallance, E., Schafner, K. J., Engles, K. J., Batchelor, T. P., Goldsmith, W. T., Wix, K., Hussain, S., & Nurkiewicz, T. R. (2022). Nanomaterial inhalation during pregnancy alters systemic vascular function in a cyclooxygenase-dependent manner. *Toxicological Sciences*, 188(2), 219–233.
38. Tsao, C. W., Aday, A. W., Almarzooq, Z. I., Anderson, C. A., Arora, P., Avery, C. L., Baker-Smith, C. M., Beaton, A. Z., Boehme, A. K., Buxton, A. E., & Commodore-Mensah, Y. (2023). Heart disease and stroke statistics—2023 update: A report from the American heart association. *Circulation*, 147(8), e93–e621.
39. Rajendran, A., Minhas, A. S., Kazzi, B., Varma, B., Choi, E., Thakkar, A., & Michos, E. D. (2023). Sex-specific differences in cardiovascular risk factors and implications for cardiovascular disease prevention in women. *Atherosclerosis*, 384, 117269.
40. Okoye, C. N., Koren, S. A., & Wojtovich, A. P. (2023). Mitochondrial complex I ROS production and redox signaling in hypoxia. *Redox Biology*, 67, 102926.
41. Grivennikova, V. G., & Vinogradov, A. D. (2013). Partitioning of superoxide and hydrogen peroxide production by mitochondrial respiratory complex I. *Biochimica et Biophysica Acta*, 1827(3), 446–454.
42. Clements, R. T., Terentyeva, R., Hamilton, S., Janssen, P. M. L., Roder, K., Martin, B. Y., Perger, F., Schneider, T., Nichtova, Z., Das, A. S., Veress, R., Lee, B. S., Kim, D. G., Koren, G., Stratton, M. S., Csordas, G., Accornero, F., Belevych, A. E., Gyorke, S., & Terentyev, D. (2023). Sexual dimorphism in bidirectional SR-mitochondria crosstalk in ventricular cardiomyocytes. *Basic Research in Cardiology*, 118(1), 15.
43. Zhao, Q., Sun, Q., Zhou, L., Liu, K., & Jiao, K. (2019). Complex regulation of mitochondrial function during cardiac development. *Journal of the American Heart Association*, 8(13), e012731.
44. Khalifa, A. R., Abdel-Rahman, E. A., Mahmoud, A. M., Ali, M. H., Noureldin, M., Saber, S. H., Mohsen, M., & Ali, S. S. (2017). Sex-specific differences in mitochondria biogenesis, morphology, respiratory function, and ROS homeostasis in young mouse heart and brain. *Physiological Reports*. <https://doi.org/10.14814/phy2.13125>

Publisher's Note Springer Nature remains neutral with regard to jurisdictional claims in published maps and institutional affiliations.